2D and 3D Potential Field Mapping and Modelling at the Fallon FORGE site, Nevada, USA

Jeffrey B. Witter[1], Jonathan M.G. Glen[2], Drew L. Siler[2], Dominique Fournier[3]

[1]Innovate Geothermal Ltd., Vancouver, British Columbia, Canada

[2]USGS, Menlo Park, California, USA

[3]University of British Columbia, Vancouver, British Columbia, Canada

Keywords

Geothermal exploration, gravity, magnetic, forward & inverse modelling, Fallon FORGE

ABSTRACT

Accurate geological characterization of Fallon FORGE is important for preparing the site as an EGS laboratory. As part of this effort, a 3D geologic map was constructed previously from well logs, surface geologic mapping, 2D seismic profiles, interpreted gravity & magnetic maps, and a gravity-inferred basement surface. In this study, we have conducted both 2D and 3D modelling of high-resolution gravity and magnetic data (pre-existing and new) in an effort to further refine and test this 3D geologic map at Fallon. This effort enabled a direct comparison of the 2D and 3D model results. Potential field modelling was guided by rock-property measurements of samples from drill-core and outcrop from the Fallon area. In total, five 2D potential field model profiles, up to 30 km in length, were constructed that extend across the Fallon area. The 3D gravity model volume was 8 km (N-S) x 8 km (E-W) x 4 km (thick). The majority of the 3D gravity model volume had 100 m cubic cells; but cells near the land surface were 1 m thick to adequately capture topography. Overall, the 2D & 3D geophysical modelling largely confirmed the previously constructed 3D geologic map at Fallon for three reasons: 1) lithologic boundaries in the 2D & 3D density models mostly agree with those in the 3D geologic map, 2) the rock properties used in the models lie within the range of independent measurements made on representative rock samples from the region, and 3) the match between the observed and calculated anomalies are largely within the measurement error of the observed fields. In places where the geophysical and geologic models differ, geophysical model results have revealed subsurface structural features that have helped refine geologic interpretations which, in turn, lead

to adjustments to the 3D geologic map. In this paper, we present the 2D & 3D geophysical model results and discuss how they were utilized to confirm and refine our 3D geologic understanding of the Fallon FORGE site.

1. Introduction

Potential-field (gravity and magnetic) methods can image variations in crustal density and magnetic properties, even when those variations are concealed beneath overburden. Variations in physical properties manifest from a variety of tectonic and magmatic structures and processes, including faults, folds, fractures, basins, intrusions, hydrothermal alteration, and lateral facies changes. Gravity and magnetic anomalies arising from physical-property variations can be mapped, modeled, and interpreted in order to improve understanding of subsurface geology and its tectonic and magmatic history, particularly when interpretations are combined with other geophysical methods and geologic constraints.

Potential field methods are useful in geothermal settings because they commonly highlight structural features that may play a role in guiding geothermal fluids or that may be activated during stimulation of a geothermal field. Potential-field methods are particularly useful in areas throughout the northwestern Great Basin, where physical properties of the Mesozoic basement or mafic-intermediate volcanic and intrusive rocks contrast strongly with the surrounding tuffaceous and sedimentary rocks to produce prominent gravity and magnetic anomalies. These methods also may be used to map alteration and hydrothermal deposits, where geothermal fluid flux results in characteristic changes to the density and rock-magnetic properties.

In the Fallon FORGE study area (Figure 1), contrasts between basin fill, volcanic rocks, and Mesozoic basement rocks generate a distinguishable pattern of gravity and magnetic anomalies that can be used to infer subsurface geologic structure. In Phase I of the Fallon FORGE project, existing gravity and aeromagnetic data were analyzed to assess regional crustal structures and aid in development of the initial Fallon three-dimensional (3D) geologic map. Sources of data employed in the Phase I investigation included a gravity database of nearly 8000 gravity stations and a regional aeromagnetic compilation. In Phase II of the Fallon FORGE project, we established over 900 additional gravity stations, collected new ground-magnetic measurements, and conducted potential-field modelling along several profiles across the study area in order to better constrain subsurface structure.

This paper accomplishes several tasks. First, we describe the new gravity, magnetic and rock-property data collected in Phase II of the Fallon FORGE project. Second, a map-based interpretation of the gravity and magnetic data is discussed in the context of understanding the structural geology at Fallon. Third, the results of two-dimensional (2D) joint gravity and magnetic modelling along profiles is described. Fourth, the outcome of geologically-constrained, 3D inversion modelling of gravity data is presented. Lastly, we directly compare the 2D profile models and 3D inversion model to explore the similarities and differences encountered when using either of these two methods.

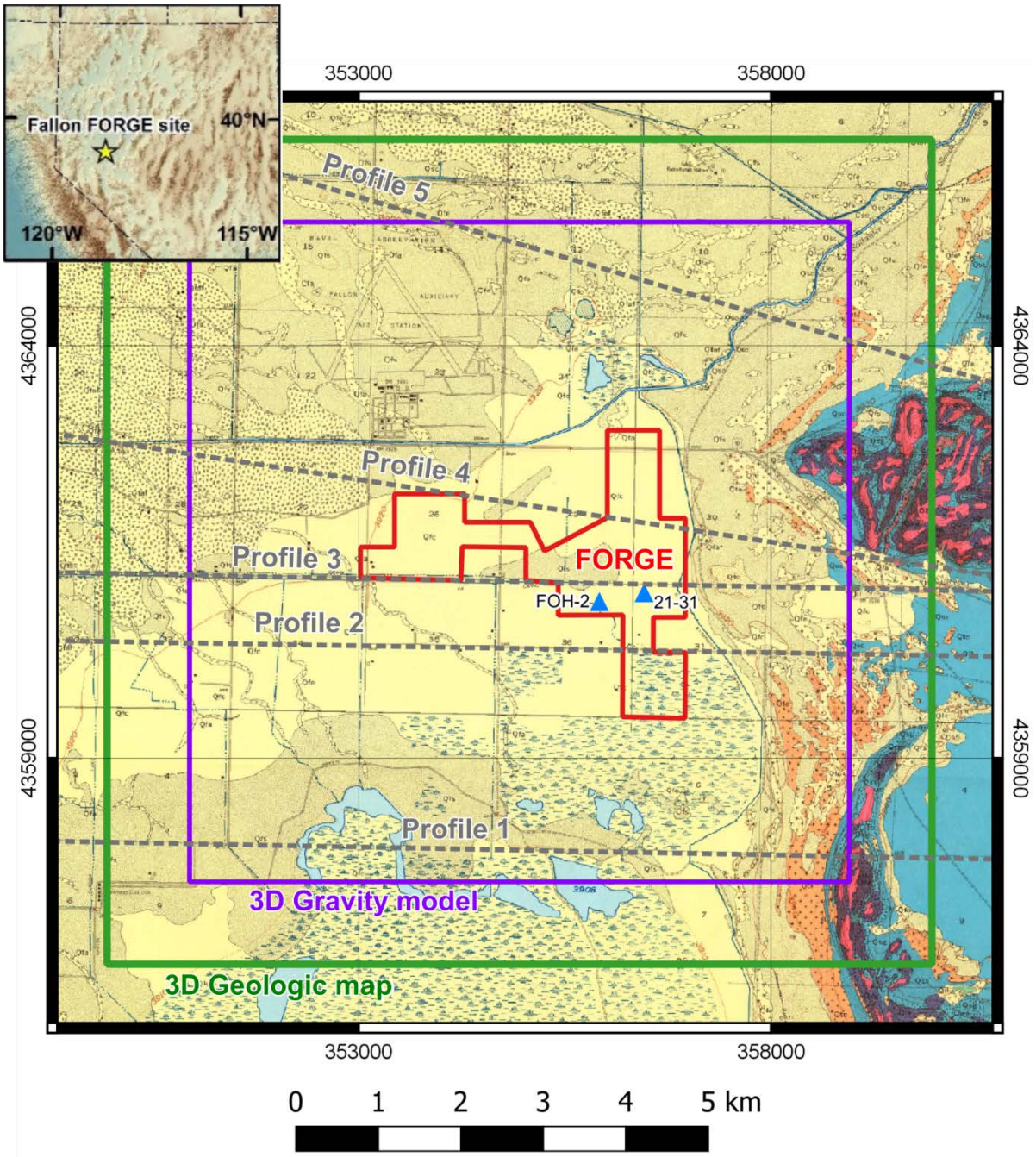

Figure 1: Location map of the project area. Fallon FORGE footprint (red polygon), Fallon 3D geologic map footprint (green box), 3D gravity model footprint (purple box), and high resolution 2D potential field profiles (grey dashed lines) are shown. Locations of two deep wells mentioned in the text are also indicated (blue triangles). Background image is the surface geologic map of the area from Morrison (1964). Red colors on the geologic map represent surface exposures of Tertiary mafic volcanic rocks; all other rock units exposed at the surface are Quaternary sedimentary units. Coordinates are in UTM NAD83 zone 11. Inset shows the location of Fallon in western Nevada. FORGE = Frontier Observatory for Research in Geothermal Energy and is a program supported by the U.S. Department of Energy

2. Gravity Data

A database of nearly 8000 existing gravity stations spanning a ~130 x 130 km area centered on the Carson Sink was compiled from a variety of public domain and privately contracted databases (Blankenship et al., 2016), including a proprietary, high-resolution survey consisting of a 200-m grid of stations covering the eastern portion of the proposed FORGE site.

In order to fill gaps in the existing data coverage, over 900 additional gravity stations (Figure 2) were collected. These new data provide a dense station coverage on the west side of the FORGE site (Figure 2), and increase the density of gravity stations along seismic lines or other key profiles. However, the spatial distribution of the new data collection was locally limited by private lands, cultural features that inhibit ground traverses (e.g., fences, canals), and wetlands.

The new gravity data were collected along roads and, where possible, in a grid pattern with station spacings ranging between 150 – 300 m. Observed gravity values for previous and newly collected data were combined into one dataset and reduced to isostatic residual gravity anomalies using standard gravity methods (Blakely, 1995) that correct for multiple parameters, including earth tides, instrument drift, latitude, elevation, Earth curvature, terrain and an isostatic correction that corrects for deep sources that isostatically support topographic loads.

The combined existing and new dataset spanning the FORGE footprint provide a remarkably good station coverage over most of the 3D geologic map extent (consisting largely of a 250-300 m station grid). Exceptions to this occur over the southwest part of the 3D model area, where access was limited (Figure 2). Outside the 3D geologic map area, data coverage is more heterogeneous, but newly acquired profile data provide detailed constraints along key seismic profiles (extending east of the 3D model area). In places where gravity stations are sparse, structural interpretations are less-well constrained. However, even in the southwest part of the study area, where a continuous grid of data is lacking, there is sufficient data coverage to map subsurface structure. For more details regarding the Fallon FORGE gravity data, see Blankenship et al. (2016) and Siler et al. (2018).

3. Magnetic Data

The USGS collected 475 km of new ground magnetic data across the Fallon FORGE site with an emphasis on the eastern half of the 3D geologic map extent (Figure 3). Despite data gaps that reflect a lack of accessibility to private land, cultural features (e.g., fences, canals), and wetlands, this dataset provides a significant increase in resolution compared to existing regional aeromagnetic data.

The new magnetic data were collected either on foot or using tower and towed-ATV (all-terrain vehicle) magnetometer systems (Athens et al., 2011). A stationary proton-precession magnetometer was used to record and correct for temporal variations of the Earth's magnetic field during the surveys. Additional processing removed anomalies associated with cultural "noise," such as cars, culverts, fences, and power lines.

In addition to these new data, a proprietary ground magnetic survey was made available for use in this study (Blankenship et al., 2018). New and existing surveys were leveled and merged to

form a single, high-resolution magnetic dataset with lines spaced <200m over most of the eastern half of the study area. Additional details of the Fallon FORGE magnetic data can be found in Siler et al. (2018).

4. Rock Property Data

Knowledge of rock density and magnetic properties is essential for deriving accurate potential-field models of subsurface geology. Density (dry bulk, grain, and saturated bulk densities), magnetic susceptibility, and remanent magnetization measurements were made on drill cores and on paleomagnetic samples taken from nearby regions with lithologies relevant to the FORGE study area. Density and magnetic susceptibility measurements were also performed on core samples obtained from three wells: 51-20 (~6 km SE of the FORGE site), FOH-2 (within the FORGE area), and BCH-3 (at the Bradys geothermal area ~70 km NW of the FORGE site), that span a variety of Tertiary volcanic and Mesozoic basement lithologies.

4.1 Density Data Collection

Densities were determined for 325 samples from the three drill cores using a precision electronic balance. All rocks were weighed three times: dry in air (Wa), saturated and in water (Ww), and saturated and in air (Ws). From these three weights, grain density (D1), dry bulk density (D2), and saturated bulk density (D3) were calculated for each sample using simple formulae:

- D1 = Wa/(Wa-Ww) grain
- D2 = Wa/(Ws-Ww) dry bulk
- D3 = Ws/(Ws-Ww) saturated bulk

Saturated measurements were performed after samples had soaked in water for 24 hours. Saturated-in-air weights were made upon immediate removal of the sample from water.

4.2 Magnetic Susceptibility Data Collection

Volume corrected apparent magnetic susceptibilities were determined for 317 drill core segments using an MS3 sensor and passing core segments through an MS2C (80 cm diameter) coil. Susceptibility readings, determined for 40 paleomagnetic samples, were performed using a Bartington MS3 meter equipped with an MS2B sensor.

4.3 Magnetic Remanence Data Collection

A suite of paleomagnetic samples were provided for this study (Blankenship et al., 2018). Remanent magnetization data were acquired for 93 samples spanning 11 sites (individual flows) from a middle Miocene basaltic andesite volcanic section within the Bunejug Mountains (just outside the SE corner of the Fallon 3D geologic map area). All sites in the Bunejug Mountains are reversely magnetized and yield an in-situ section mean direction with a declination of 153° and inclination of -30°.

4.4 Synopsis of Rock Density Analysis for Gravity Modelling

The subsurface geology at the three wells from which the density data were obtained consists of Quaternary sediments (Qs), Quaternary-Tertiary sediments (QTs), mafic Tertiary volcanic rocks (Tvs), and a variety of Mesozoic basement rocks (Mzu). Density measurements were made only on the Tvs and Mzu rock types encountered in the wells (Table 1). Density measurements of the Quaternary and Tertiary sedimentary cover (Qs & QTs) were not performed because the unconsolidated nature of these rocks made laboratory density measurements not possible. However, geologically-reasonable densities for Qs and QTs lie in the range 1.9 – 2.3 g/cm^3.

Table 1. Summary of rock density measurements from core in three wells on or near the Fallon FORGE site.

Well	Rock unit	Number of measurements	Average Saturated Bulk Density (± 1σ SD)
51-20	Tvs	33	2.419 ± 0.138 g/cm^3
FOH-2	Tvs	172	2.410 ± 0.127 g/cm^3
BCH-3	Tvs	54	2.390 ± 0.123 g/cm^3
BCH-3	Mzu	42	2.630 ± 0.40 g/cm^3

The average saturated bulk density of the mafic Tertiary volcanics (Tvs) in the three wells were weighted by the relative abundance of different rock sub-units identified within the Tvs section. Using this approach, the saturated bulk density of rock unit Tvs is 2.419, 2.410, and 2.390 g/cm^3 in wells 51-20, FOH-2, and BCH-3, respectively (Table 1). Thus, the average density for the Tvs rock unit is quite consistent from one well to the next with a value of ~2.4 g/cm^3.

The estimated saturated bulk density of the Mesozoic basement rocks found in well BCH-3 (also weighted by the observed proportions of the different rock sub-units) is 2.630 g/cm^3 (Table 1). This value is uncertain because it assumes literature values for the densities of 5 out of the 7 rock types that occur in the basement. Additional density measurements of basement rocks are needed to better constrain this value.

5. Gravity and Magnetic Maps

Gravity and magnetic data were processed using routines available in Oasis Montaj® software. New and existing data were merged and gridded at 100 m spacing using minimum curvature interpolation to produce grids of the isostatic gravity and total magnetic field anomalies that reflect variations in the distribution and character of subsurface rock-properties and help to reveal the geometry of major rock units and structures across the greater-FORGE study area (Figures 2 & 3). We also applied a variety of derivative and filtering methods to these grids to aid in interpretation by helping to delineate structures, such as buried faults or contacts.

Figure 2 shows isostatic anomalies that have been filtered in order to emphasize shallow sources; i.e., the isostatic anomaly grid was continued upward 500 m and subtracted from the original grid. Shallow-source gravity anomalies aid in identifying near-surface faults and contacts.

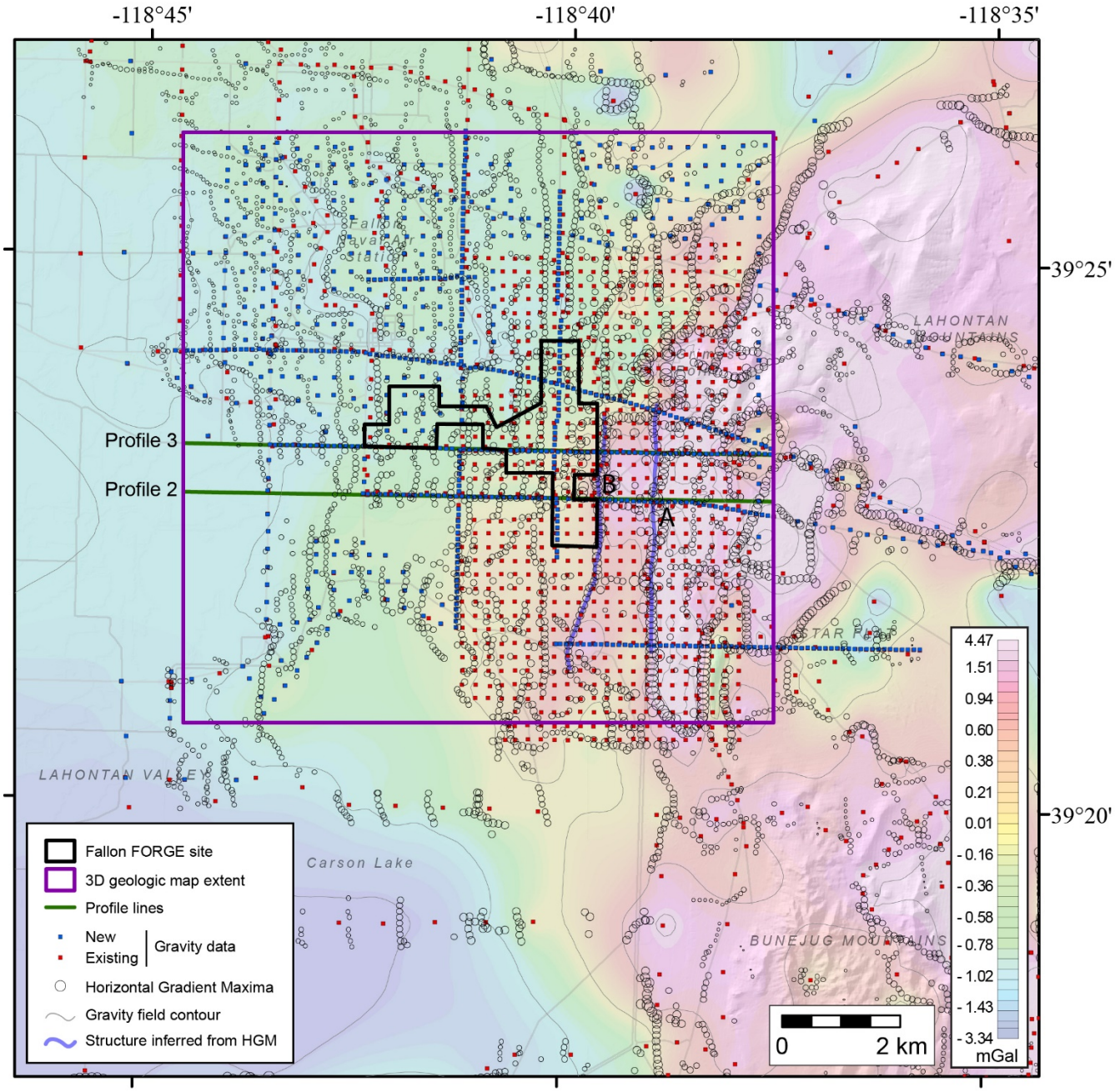

Figure 2: Colored isostatic residual gravity and shaded topographic relief map of the Fallon FORGE project area showing horizontal gradient maxima (HGM) of isostatic gravity. HGM are shown as strings of circles. Two prominent structural features inferred from continuous HGM are highlighted in purple (labeled A, B) and discussed in Figure 4.

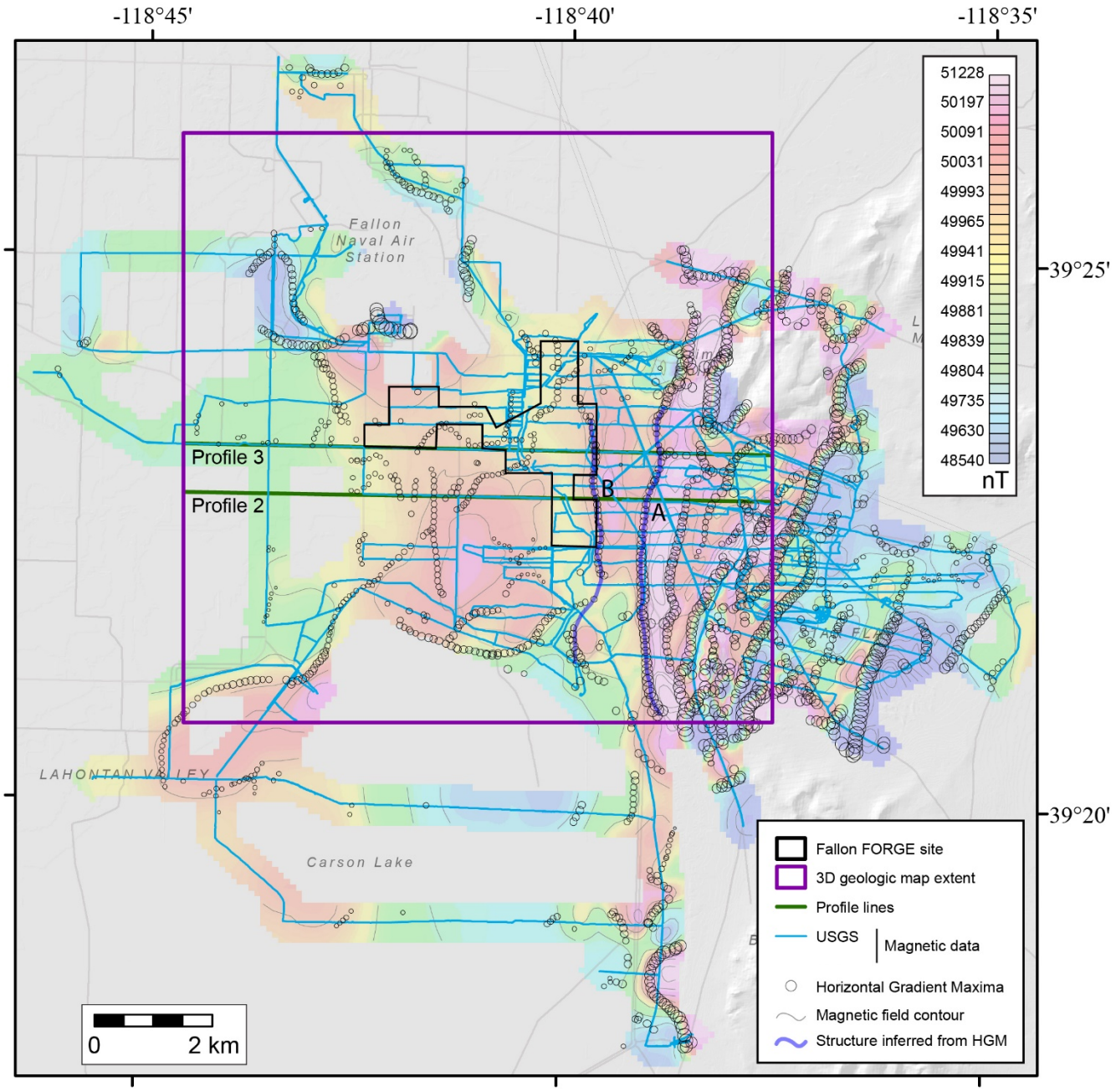

Figure 3: Colored residual reduced-to-pole magnetic anomaly and shaded topographic relief map of the Fallon FORGE project area showing horizontal gradient maxima (HGM) of pseudogravity. HGM are shown as strings of circles. Two prominent structural features inferred from continuous HGM are highlighted in purple (labeled A, B) and discussed in Figure 4.

Reduced-to-pole (RTP) and pseudogravity anomalies (Blakely, 1995) are generated from the total field magnetic anomaly grid in order to facilitate evaluation of anomaly sources. RTP, which is a method that converts the magnetic anomaly to one that would be observed if the magnetization were vertical was used to generate the anomaly map shown in Figure 3. The pseudogravity transform converts a magnetic anomaly into the gravity anomaly that would be

observed if the magnetic distribution of the body were replaced by an identical density distribution. This transformation simplifies interpretations in several ways. First, it removes the edge effects associated with magnetic anomalies. Second, it centers the anomalies over their causative sources, thereby delineating the lateral extent of sources. Third, it allows for a more direct comparison with actual gravity anomalies.

Locally steep gradients in potential field anomalies are indicative of subsurface structure. For example, the location of maxima in the horizontal gradients (HGM) of gravity and pseudogravity anomalies overlie abrupt lateral changes in density or magnetization, respectively, which is useful in estimating the lateral extent of buried sources (Blakely and Simpson, 1986). This method assumes that lateral changes in physical properties occur at vertical contacts. Dipping contacts will shift the mapped location slightly in the direction of dip. Local HGM were calculated for both isostatic gravity and pseudogravity grids (Figures 2 & 3).

6. 2D Potential Field Profile Modelling

Potential field modelling is inherently non-unique and therefore integrating constraints from other datasets is an important part of the modelling process. Joint gravity and magnetic modelling, integrated with drill-hole information and analysis of the reprocessed seismic reflection sections, provided key geologic cross-sections along several profiles across the FORGE area that informed the 3D geologic map.

2D potential field models were developed along five profiles across the study area (Profiles #1-5; Figure 1). Portions of two of these profiles, where they cross the FORGE footprint, are shown in Figure 4. Modelling was performed using commercially available software (GM-SYS®). This employs standard forward modelling methods (Talwani et al., 1959; Blakely and Connard, 1989) that approximate subsurface geology with horizontal tabular prisms that are characterized in the 2D cross-section as model blocks. The model blocks were constrained to be consistent with mapped geologic units. The geometries of the model bodies were determined through a series of forward and inverse calculations (whereby density and magnetic properties of 2D bodies were adjusted iteratively) to match model anomalies with observed anomalies within the limits imposed by surface geology, rock property data, and HGM that are useful for estimating the horizontal extent of buried sources.

Although potential field models are relatively effective at constraining the depth to the top of an anomaly source or the location and dip of its edges, they are relatively insensitive to the depth of the base of a source and therefore characterize the shallow and deeper crust with different degrees of detail. In addition, potential field models are critically dependent on the modelling assumptions inherent in the simplification of complex geology by discrete geometric blocks. For the most part, profile models are oriented perpendicular to the strike of geologic units or structures of interest. In places that are inherently 3D in structural or geologic character, the 2D modelling may not adequately reflect the subsurface. In these cases, misfit between observed and calculated potential field anomalies is expected, and 3D modelling may be warranted.

We generated five geologic cross-sections, four of which approximately coincide with the location of reprocessed and reinterpreted seismic lines that cross the 3D geologic map area. In

each cross-section, three primary geologic rock types are modeled: the basin sedimentary section, the underlying volcanic section, and the basement section. Model units are assigned unique density and magnetic properties based on the measured data discussed previously (see Section 4), as well as data derived from a national database (unpublished data, D. Ponce, USGS, 2016) consisting of over 19,000 measurements made on lithologies similar to those in the study area. In addition, both the sedimentary and volcanic sections are separated into four regionally-horizontal internal units, whose properties increase in density with depth to reflect typical density-depth relations found throughout Nevada (Jachens and Moring, 1990). Uncertainties in the local density-depth model should primarily affect the predicted cover thickness, but the interpretation of the location and geometry of structures should be relatively insensitive to these uncertainties.

Magnetic anomalies depend on both the induced magnetization and remanent magnetization of subsurface volcanic rocks. The strength of the induced magnetization, which is proportional to the magnetic susceptibility, was assigned a constant value for all model bodies representing the same unit. Remanent magnetization, on the other hand, varied for each volcanic unit, according to available data. A reverse magnetization is assigned to the shallowest volcanic layer and is based on results derived from paleomagnetic measurements performed on samples obtained from outcrops in the Bunejug Mountains. Remanent magnetization assigned to deeper volcanic units was assumed to be normally magnetized in the direction of a Geocentric Axial Dipole (GAD) field. This assumption was made due to the lack of direct measurements on those units and because deeper, older volcanic units are likely to have significant viscous remanent magnetization that reflects the time-averaged GAD magnetic field over the last normal polarity epoch.

Potential field modelling helps constrain the shape and location of subsurface structures and contacts that reflect contrasts in rock properties. The best constraints are provided on shallow structural features involving sedimentary/volcanic contacts, as well as the interface between volcanic rocks and the crystalline basement. Prominent features are particularly well-constrained on the eastern side of the study area, where volcanic and basement rocks occur at relatively shallow depths.

7. 3D Modelling of Potential Field Data

7.1 3D inversion Modelling of Gravity Data

We employed 3D geophysical inversion modelling of gravity data to generate a 3D density model for the Fallon FORGE site. The goal of this effort is to independently test the 3D geologic map developed in Phase 2B (Figure 5). The 3D gravity modelling technique employed here has previously been applied successfully at the nearby Bradys geothermal area (Witter et al., 2016). The high-resolution gravity dataset at Fallon provides a uniform spatial coverage that is particularly well-suited for the application of 3D modeling. A successful test of the 3D geologic map using this 3D gravity inversion method would have the following characteristics: 1) agreement between the observed gravity measurements made at the land surface and the gravity response calculated from the output 3D density model, 2) the agreement between the observed and calculated gravity is within the error of the gravity survey measurements, 3) the 3D density

model honors the geologic horizon boundaries in the 3D geologic map, and 4) the 3D density model contains geologically reasonable density ranges for the different rock units in the 3D geologic map. Our 3D gravity modelling effort was successful at Fallon FORGE in that all four of these criteria were met. We can conclude that the 3D geologic map generated in Phase 2B is quantitatively consistent with the measured gravity data. Such consistency increases confidence that the Phase 2B geologic map is an accurate representation of the subsurface.

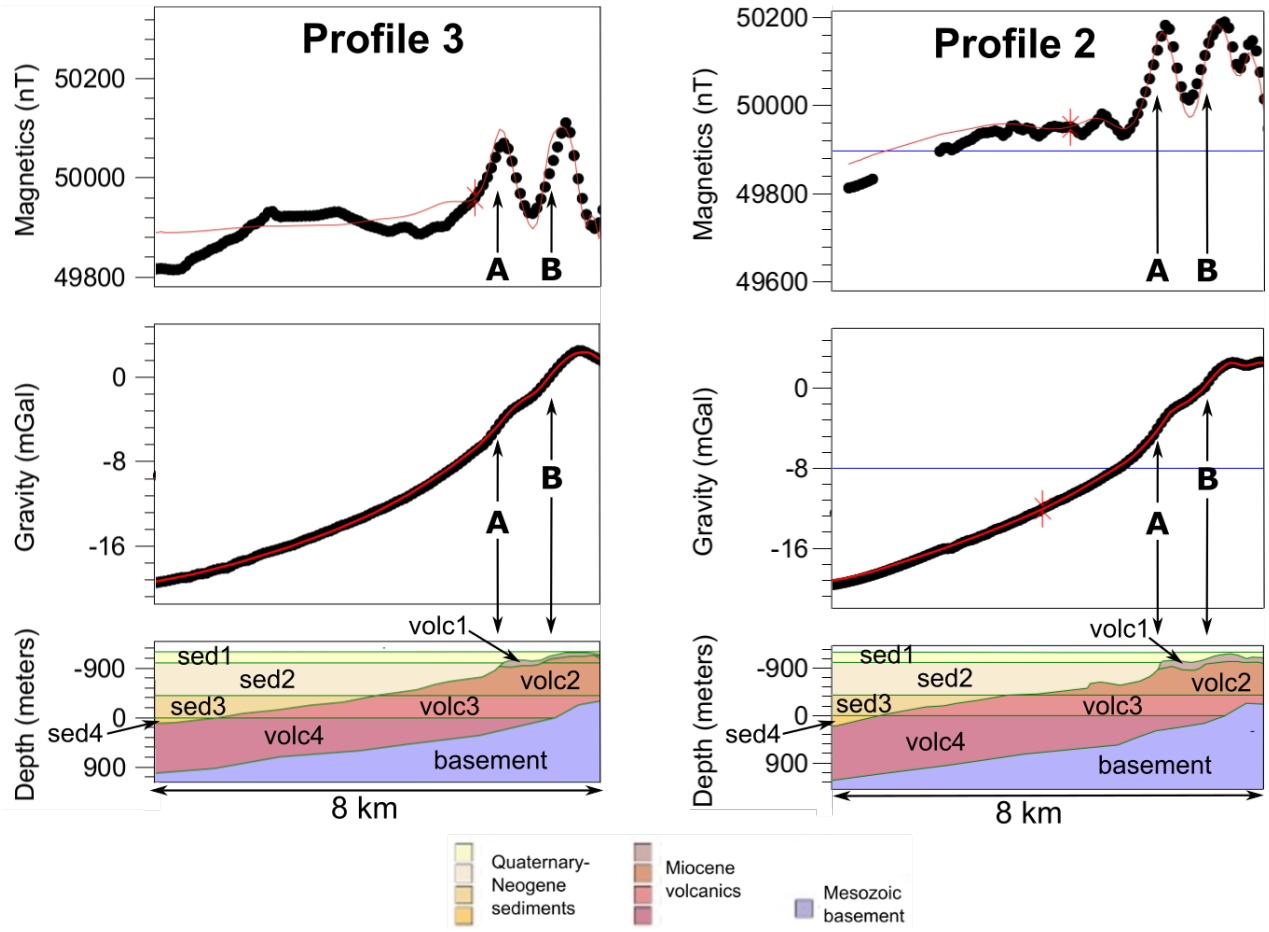

Figure 4. Two-dimensional potential field models along profile #3 (left side) and profile #2 (right side) clipped to the boundary of the 8 km wide 3D gravity model (see Figures 2 & 3 for clipped profile extents). Profiles #3 and #2 are roughly coincident with seismic lines NC744 and Navy1, respectively. The top panels show observed (black circles) and model (red line) anomalies for magnetics. The middle panels show observed (black circles) and model (red line) anomalies for gravity. The bottom panels show the potential field model with individual model bodies colored by rock unit. Sedimentary units (sed) coincide with 3D geologic units Qs and QTs; volcanic units (volc) coincide with 3D geologic unit Tvs; and the basement unit coincides with the Mesozoic 3D geologic unit Mzu. Rock properties used in the 2D models are shown in Table 2. Distinct gravity and magnetic gradients (labeled A, B) coincide with mapped structures highlighted on the magnetic and gravity maps (Figures 2 & 3).

Table 2. Potential field model properties applied to each model rock unit for 2D modelling.

Model blocks	Density (g/cm^3)	Susceptibility (SI)	Remanence (A/m)	Declination (deg)	Inclination (deg)
sed1	1900	0.002	0		
sed2	2000	0.007	0		
sed3	2200	0.005	0		
sed4	2300	0	0		
volc1r	2300	0.02	2	157	-30
volc1n	2300	0.02	2	0	60
volc2	2350	0.02	2	0	60
volc3	2400	0.02	2	0	60
volc4	2420	0.02	2	0	60
basement	2670	0.01	0		

The 3D volume used in the gravity modelling exercise has the following dimensions: 8 km (N-S) x 8 km (E-W) x 4 km (thick). This gravity model volume is centered on the Fallon FORGE site (Figure 1). The majority of the gravity model volume has 100 m x 100 m x 100 m cubic cells. Near the land surface, model cells have a thickness of only 1 m to adequately capture variations in topography.

The specific gravity data used in the 3D geophysical modelling are complete Bouguer anomaly (CBA) values (from 1282 point measurements). Of the 1318 original points in the gravity dataset, 11 were removed due to unusually high misfit and 25 duplicate datapoints were also removed. For the 3D modelling, we chose a reference density of 2.55 g/cm^3 as it approximates the bulk density of the model volume. A weak trend was observed in regional gravity data for the Carson Sink (having a magnitude of ~50 μGal/km decreasing toward the SE), and it was removed from the CBA data prior to inversion modelling. The source of this weak regional gravity trend is unknown.

The geologic horizon boundaries from the Phase 2B geologic map were used as a fixed reference in the 3D gravity modelling process. Average density values for rock units in the 3D geologic map were obtained from literature values as well as ~300 density measurements made on rock core (Table 1) from three nearby wells. These measured density values populate a starting density model, which helps to guide the gravity inversion process. We used the inversion algorithm to iteratively calculate a density distribution in the 3D model volume, which simultaneously honors the lithologic boundaries of the 3D geologic map (Figure 6). The iterations ceased when the output 3D density model generates a gravity response that matches the observed gravity measurements to a specified target misfit value (Figure 7). We used a target misfit value of 0.05 mGal, which is slightly better than the estimated overall average measurement error for the Fallon FORGE gravity dataset of 0.1 mGal. The actual misfit between the observed and calculated gravity data generated by the 3D gravity modelling is 0.043 mGal. A comparison of: A) the density ranges predicted for each rock unit by the gravity

modelling and B) density ranges derived from measurements of rock core is shown in Table 3. We used the open source SimPEG code (Cockett et al., 2015) to perform the 3D geophysical modelling.

In summary, we have utilized 3D inversion modelling of gravity data to generate a 3D density model for the Fallon FORGE site and vicinity. This density model honors the boundaries of the Phase 2B geologic map, returns rock unit density ranges in agreement with independent measurements and estimates, and achieves a match between observed and calculated gravity data to a level consistent with the gravity measurement error.

It is important to note that by passing this test it does not mean that the Phase 2B geologic map is a 100% accurate prediction of the subsurface at the Fallon FORGE site. Potential field modeling is non-unique and variations in geology that do not correspond with significant lateral variations in rock properties will not produce measurable anomalies. A detailed investigation of the spatial variation of predicted density within each rock unit is needed to determine if alternate geologic interpretations of the subsurface are plausible (i.e., interpretations that are still consistent with the observed gravity data). This is discussed in the Section 8.

7.2 3D inversion Modelling of Magnetic Data

In addition to 3D modelling of gravity data, we also attempted 3D inversion modelling of magnetic data at the Fallon FORGE site. We were not successful in this effort because of the presence of magnetic remanence in the mafic volcanic rocks (unit Tvs) that lie within the study area. The presence of magnetic remanence makes 3D inversion modelling particularly challenging because both magnitude and direction of rock magnetization must be taken into account in the inversion calculations, along with the geometry of the 3D geologic context, to achieve a viable result. Additional research is needed to overcome these challenges, and we propose to continue working on this problem in future work.

Table 3. Comparison of measured and 3D model density values for each rock unit.

Code	Rock Type	Range predicted in 3D density model (g/cm^3; 2σ Std. dev.)	Range of rock density measurements (g/cm^3)
Qs	Quaternary Alluvium	2.04 – 2.16	n.r.[1]
QTs	Quaternary – Tertiary Sediments	2.13 – 2.29	n.r.[2]
Tvs	Tertiary Volcanics	2.30 – 2.48	2.28 – 2.54[3]
Mzu	Mesozoic Basement	2.63 – 2.75	2.68 – 2.70[4]

[1] the predicted density range is geologically-reasonable for Quaternary alluvial sediments

[2] the predicted density range is geologically-reasonable for the Quaternary-Tertiary sediments, since they are older and likely more compacted than the overlying Quaternary alluvium.

[3] based upon the weighted average of all Tertiary volcanic rock density measurements (±1σ standard deviation)

[4] density measurements on rock core reported for the Mesozoic basement are only for two rock types – slate (2.68 g/cm^3) and altered basaltic andesite (2.70 g/cm^3); considering the range of lithologies present in the Mesozoic basement (e.g., quartzite, marble, granite), the density range predicted in the model (2.63 – 2.75 g/cm^3) is geologically-reasonable.

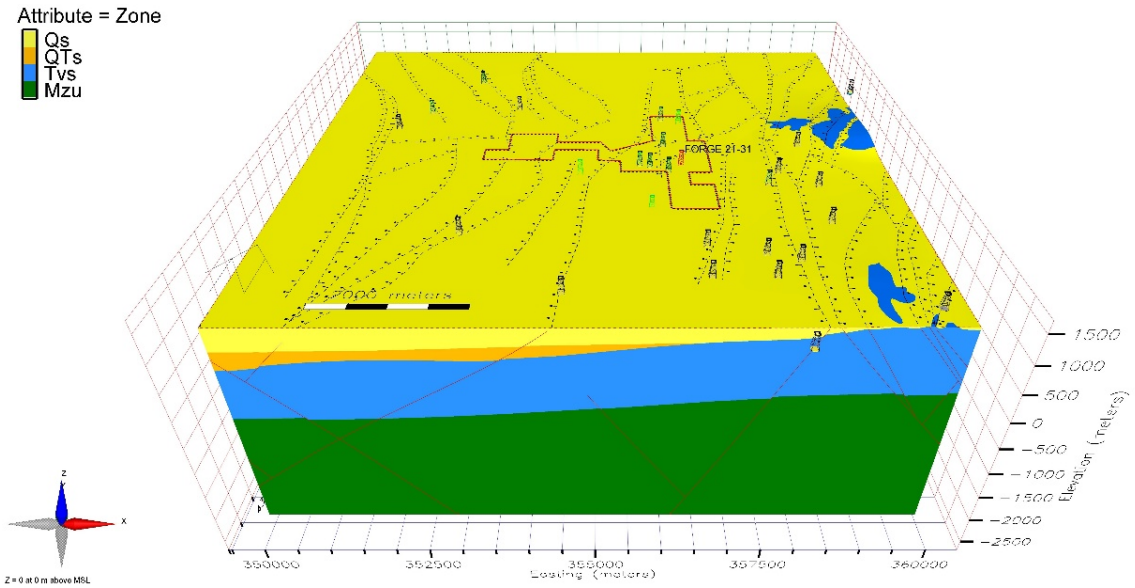

Figure 5: 3D perspective view looking north at the 10 km x 10 km x 4 km Phase 2B conceptual 3D geologic map (Siler et al., 2018). Colored rig symbols indicate the location of wells. The Fallon FORGE site is outlined in red. Green unit represents undivided Mesozoic crystalline basement rocks (Mzu); blue unit represents Miocene volcanic rocks and interbedded sedimentary rocks (Tvs); orange unit represents late Miocene to early Pleistocene (i.e., Quaternary/Tertiary) sedimentary rocks (QTs); and yellow unit represents Quaternary sediments.

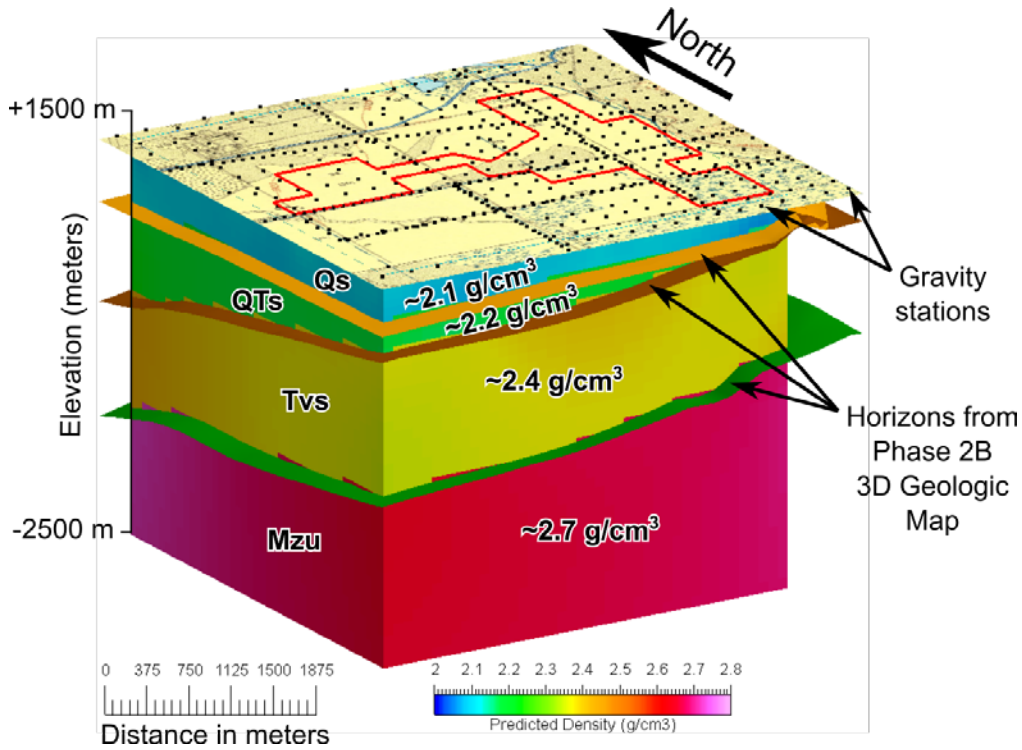

Figure 6: Perspective view to the NE of the 3D density model generated by geophysical inversion modelling of the Fallon FORGE gravity data and constrained by the Phase 2B, 3D geologic map of Siler et al., (2018). Here, the 3D density volume has been clipped to a ~5 km x ~5 km x 4 km region focused on the subsurface directly below the FORGE project area (red polygon).

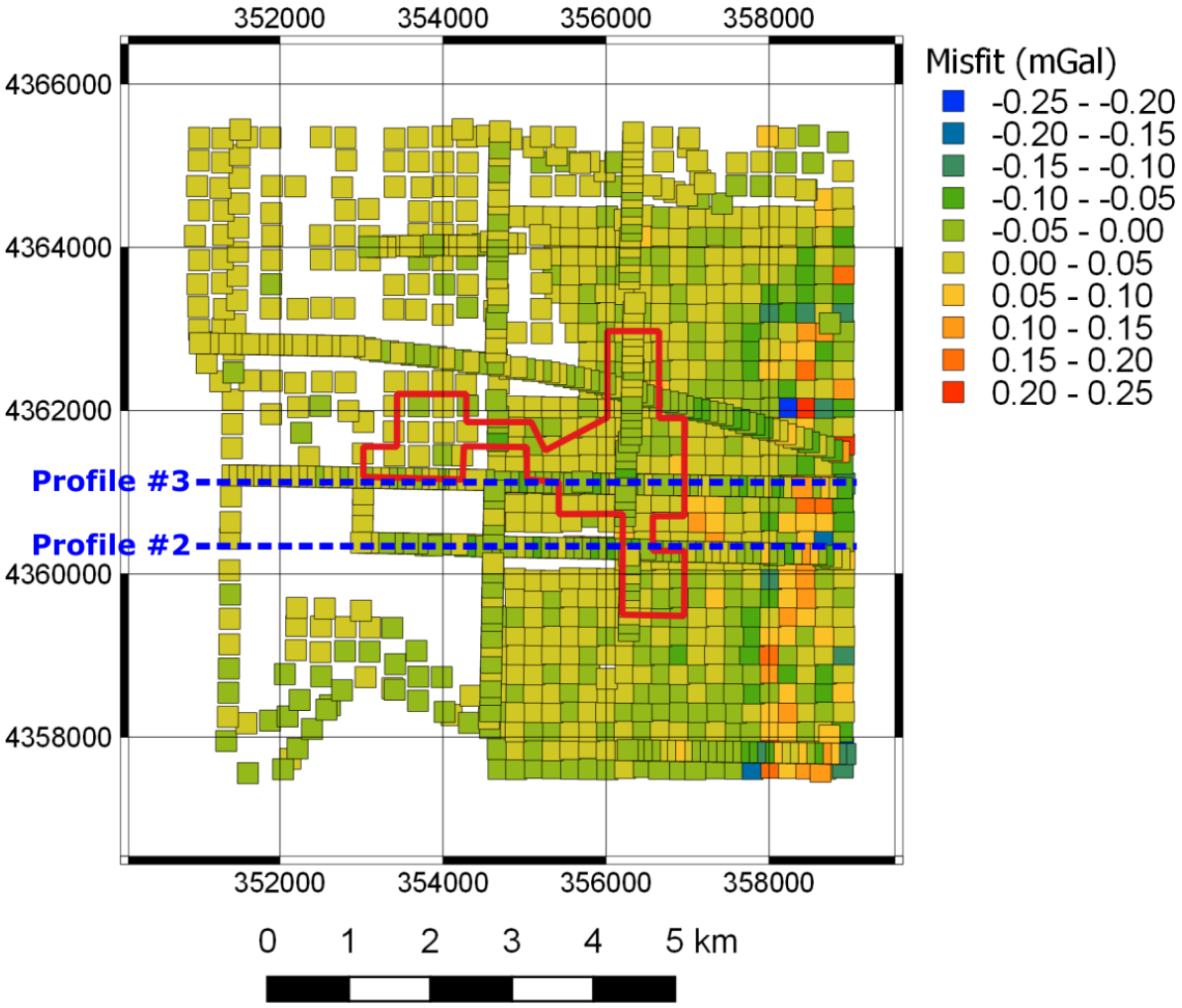

Figure 7: Plan map showing the misfit between the observed gravity data and calculated gravity response over the entire 8 km x 8 km gravity model area. Each point represents the location of a gravity measurement and is colored by the amount of misfit. The majority of the model area shows a misfit as good or better than the estimated gravity measurement error of 0.1 mGal (i.e., yellow-to-green squares). Some areas have slightly worse fit (e.g., blue and orange/red) and highlight zones which require further investigation and possibly adjustments to the 3D geologic horizon boundaries. The location of the profiles #2 and #3 in Figures 8 – 11 are shown by the dashed blue lines. Map coordinates are UTM NAD83 zone 11 in meters.

8. Discussion

The contrast in density and magnetic properties between pre-Cenozoic crystalline basement and overlying Tertiary volcanic rocks and unconsolidated basin-fill alluvium produces a distinctive pattern of gravity and magnetic anomalies. These features, when interpreted and modeled correctly, can provide valuable information pertaining to the thickness of basin sediments, depth to Mesozoic basement, and mapped location and geometry of buried faults, fracture zones, and other contacts that juxtapose contrasting geologic units at the Fallon FORGE project.

8.1 Key Elements of the Potential Field Map Interpretation

Steep gradients at several locations on the potential field maps likely indicate the presence of normal faults (e.g., A and B in Figures 2, 3, & 4). Some of these gradients correspond to mapped Quaternary faults, but others likely indicate intra-basinal faults observable only through geophysical methods. In the Fallon FORGE study area, faults can be discerned in map view by following traces of the HGM of the gravity anomaly (Figure 2). Along the range front of the Lahontan Mountains east of the study area, the gradients show continuous traces of subparallel, north-trending structures. The semi-continuous behavior of the gradients highlights their through-going nature and lateral extent. Many of these same features are reflected in the pseudogravity gradients (Figure 3). Two prominent, spatially coincident gravity and magnetic features inferred from the HGM are highlighted on Figures 2 and 3, respectively.

A north-northeast trending structural grain is particularly apparent in the eastern half of the 3D geologic map area. A general lack of prominent HGMs characterizes the western half of the 3D model extent and most of the FORGE area. This is undoubtedly due in part to the decrease in anomaly amplitudes as the depth to volcanic and basement units increases westward. However, the absence of continuous subtle gradients, where detailed data are present, suggests a lack of prominent faulting accommodating any significant displacement, which is compatible with the lack of significant faults observed in the seismic reflection data (Blankenship et al., 2018).

8.2 Comparison of 2D and 3D Density Models

Here, we discuss the differences between the 2D and 3D modelling efforts through a direct comparison. To do so, we compare a vertical slice, coinciding with profile #3, that has been extracted from the 3D density model (Figure 8) with the output of 2D potential field model profile #3 (Figure 9). Similarly, we compare a 3D density model slice along profile #2 (Figure 10) with the output of 2D potential field model profile #2 (Figure 11).

Overall, the results are quite similar using either the 2D or 3D modelling approach. For example, model densities and the locations of geologic horizon boundaries are similar in both cases and for both profiles. Furthermore, in both 2D and 3D for profiles #2 and #3 there is good agreement between the observed gravity data and that calculated for the models (see Figures 4 & 7).

Some of the differences in the 2D and 3D model results arise from the different strategies used in each of the two methods. First, the horizon boundaries from the Phase 2B 3D geologic map match exactly with the specific rock unit density contrasts in the 3D model because geologic horizon boundaries were imposed as an unmovable “hard” constraint in the 3D inversion algorithm (Figures 8 & 10). In the 2D profile models, no such “hard” constraint was imposed which explains why the geologic horizons in the 2D profile models are slightly offset from the

Phase 2B geologic map horizons (Figures 9 & 11). Moveable geologic horizon boundaries in the 2D model case helped achieve agreement between the model response and the observed data. In addition, the 2D models involved joint gravity/magnetic modeling, honoring both the observed gravity and magnetic anomalies. As a result, some structural features that occur in the 2D models (which are also largely driven by the magnetic signal) will not appear in the 3D model.

Second, both the 2D and 3D models allow for variable density within a rock unit. In the 2D case, rock density is increased in a step-wise manner in the vertical direction to mimic typical depth-density relationships in the subsurface. These step-wise demarcations in density within a rock unit are not real and are somewhat arbitrary, yet they are an important feature to include to make the 2D model more geologically realistic. Lateral variations in rock unit density have not been included in the 2D profile models.

In the 3D models, vertical variation in density is not explicitly defined as it is in the 2D models. However, density variation within rock units is allowed and is a key aspect of the 3D model output. Specifically, variations in rock unit density that fall outside expected values in the 3D model are an important indicator that the nearby geologic horizon boundaries may need to be modified. For example, the two X's in Figure 8 point to regions of the Tertiary volcanic unit (Tvs) which are predicted to have unusually high density (i.e., ~2.5 g/cm^3 model density as opposed to the expected average value of ~2.4 g/cm^3 based on density measurements; Table 1). This unusually high density can be corrected by raising the Top-Tvs horizon boundary by a small amount (i.e., far enough until the average density in that portion of the Tvs rock unit reaches

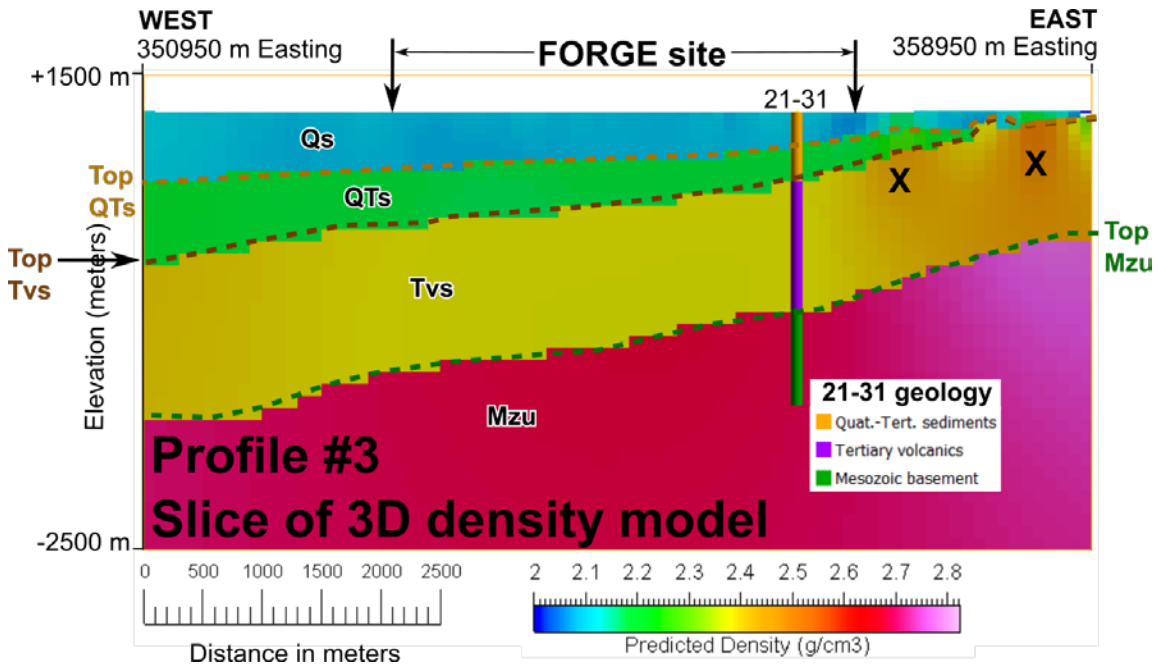

Figure 8: An E-W trending, 8 km wide, vertical cross-section through the 3D density model (along Profile 3; see Figure 7 for location) which shows different model densities for each of four stratigraphic layers as well as subtle lateral variations in density within each stratigraphic layer. 3D model density values are shown by the color bar in g/cm^3. The dashed lines show the horizon boundaries of the Phase 2B geologic map dipping down to the west. Downhole geology from well 21-31 (offset 100 m south of profile) is also shown.

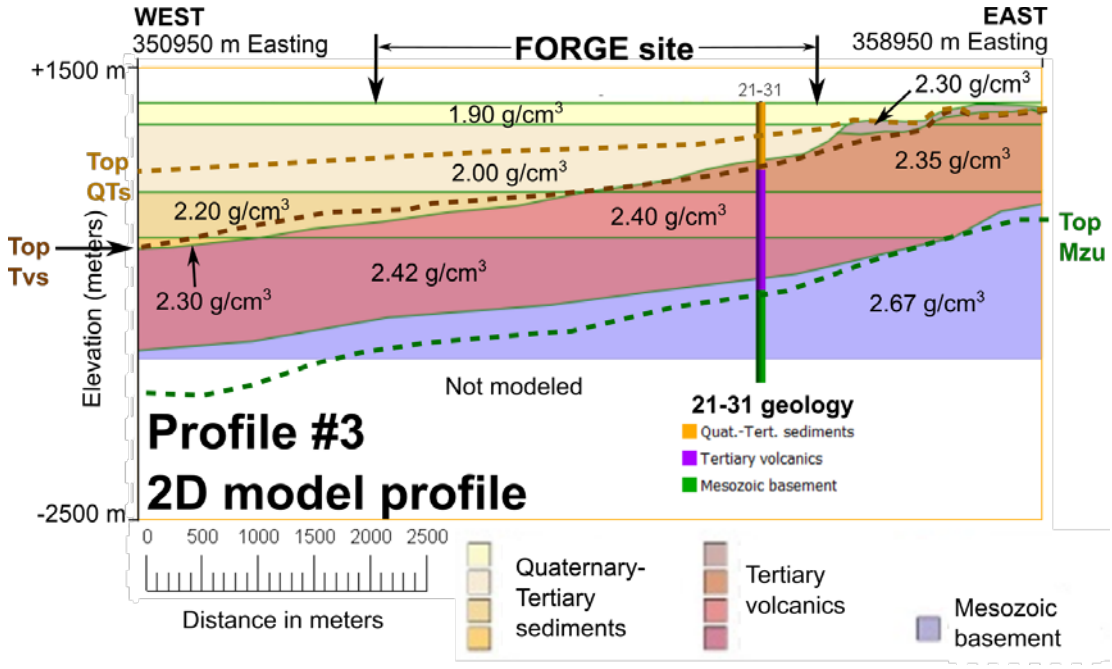

Figure 9: E-W trending, 8 km wide, 2D potential field profile model #3 (location shown in Figure 7) which shows distinct model densities for different stratigraphic layers but also contains vertical density gradations within stratigraphic layers. The dashed lines show the horizon boundaries of the Phase 2B 3D geologic map for comparison. Downhole geology from well 21-31 (offset 100 m south of profile) is also shown.

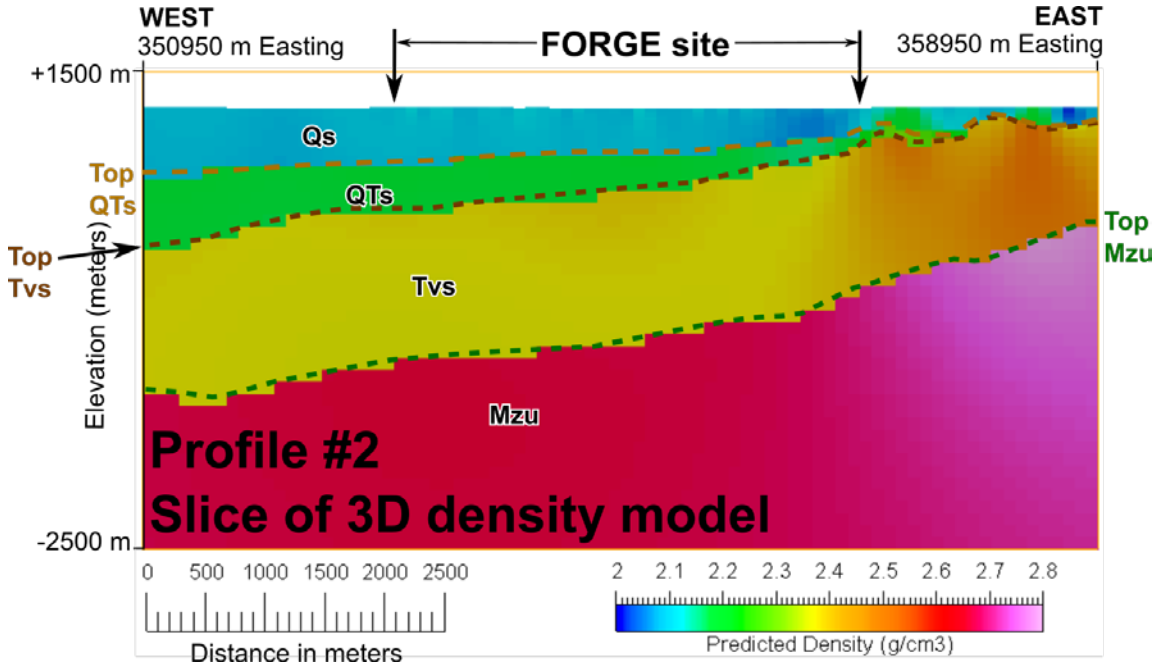

Figure 10: An E-W trending, 8 km wide, vertical cross-section through the 3D density model (along Profile 2; see Figure 7 for location) which shows different model densities for each of four stratigraphic layers as well as subtle lateral variations in density within each stratigraphic layer. 3D model density values are shown by the color bar in g/cm^3. The dashed lines show the horizon boundaries of the Phase 2B 3D geologic map dipping down to the west.

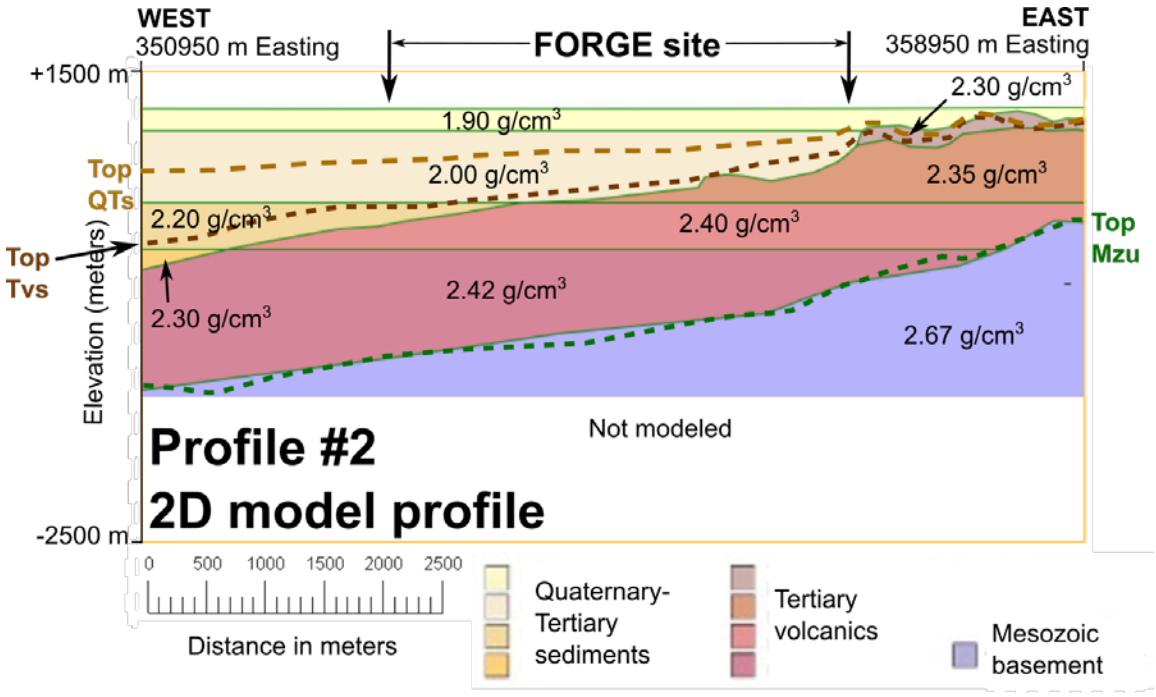

Figure 11: E-W trending, 8 km wide, 2D potential field profile model #2 (see Figure 7 for location) which shows distinct model densities for different stratigraphic layers but also contains vertical density gradations within stratigraphic layers. The dashed lines show the horizon boundaries of the Phase 2B 3D geologic map for comparison.

~2.4 g/cm^3). A similar argument can be made for raising the Top-Mzu horizon boundary by a small amount on the east side of the 3D profiles to alleviate unusually high densities in that region (i.e., model densities of ~2.75 g/cm^3 (pink) when the expected density is ~2.7 g/cm^3).

In practice, 2D and 3D potential field modelling are methods which are complementary to one another. Multiple 2D profile models are particularly valuable to aid in the initial construction of a comprehensive 3D geologic map. The 2D profile approach can suffer, however, in regions with strongly 3D geology. Furthermore, construction of a large number (e.g., dozens) of 2D profiles to fill a 3D volume would be overly-laborious. Modelling of gravity data in 3D is also valuable because it is not impeded by 3D geology and creates a density model that completely fills the 3D model volume. 3D gravity modelling is best suited to exploration projects where a 3D geologic map has already been constructed so that the gravity inversion result can be used to test and update the 3D geology. Applying 3D gravity inversion modelling to a region with completely unknown geology is challenging because of the abundance of undefined parameters (e.g., location, shape, and density of geologic bodies). In general, fully unconstrained 3D gravity inversion modelling (i.e., where neither 3D geology nor rock property values are used to guide the inversion) is not recommended as the results can be non-geological and misleading.

9. Conclusions

Potential field modelling, along 2D profiles or as 3D rock property volumes, is a valuable geothermal exploration tool to characterize and test the geologic framework of the subsurface. In this study, we show that potential field mapping and modelling has helped define and refine the 3D geologic map at the Fallon FORGE site, Nevada. Successful potential field model results were obtained by employing both geological constraints and rock property measurements to guide the modelling process. A direct comparison between the 2D and 3D potential field models revealed similar results, irrespective of the modelling method. Differences between the 2D and 3D results arose due to differences in input parameters and modelling strategy. Some differences may also reflect 3D source-geometries that are not adequately characterized and modeled by 2D bodies. Future work includes incorporation of additional rock density data from analogue surface rock samples and a wireline geophysical log as well as 3D magnetic modeling that accounts for remanence.

Acknowledgments

Many thanks to Geoff Phelps of the USGS for his expert data processing and compilation of the gravity and magnetic datasets used in this study.

REFERENCES

Athens, N.D., Glen, J.M.G., Morin, R.L., and Klemperer, S.L., 2011, ATV magnetometer systems for efficient ground magnetic surveying: The Leading Edge, v. 30, p. 394–398, doi: 10 .1190 /1 .3575284.

Blakely, R.J., 1995, Potential theory in gravity and magnetic applications: New York, Cambridge University Press, 441 p.

Blakely, R.J., and Connard, G.G., 1989, Crustal studies using magnetic data, in Pakiser, L.C., and Mooney, W.D., eds., Geophysical framework of the continental United States, Geological Society of America Memoir 172, p. 45-60.

Blakely, R.J., and Simpson, R.W., 1986, Approximating edges of source bodies from gravity or magnetic data: Geophysics, v. 51, p. 1494–1498, doi: 10.1190/1.1442197.

Blankenship, D., Akerley, J., Blake, K., Calvin, W., Faulds, J.E., Glen, J., Hickman, S., Hinz, N., Kaven, O., Lazaro, M., Meade, D., Kennedy, M., Phelps, G., Sabin, A., Schoenball, M., Siler, D., Robertson-Tait, A., Williams, C., 2016, Frontier Observatory for Research in Geothermal Energy: Phase 1 Topical Report, Fallon, NV, SANDIA National Laboratories Report SAND2016-8929, 311 p.

Blankenship, D., Akerley, J., Ayling, B., Barrow, P., Bauer, S., Blake, K., Blanksma, D., Damjanac, B., Dobson, P., Eneva, M., Faulds, J.E., Fortuna, M., Furtney, J., Glen, J., Hackett, L., Hammond, B., Hazzard, J., Bourdeau-Hernikl, J., Hickman, S., Hileman, M.,

Hinz, N., Kaven, O., Kneafsey, T., Lazaro, M., Camacho-Lopez, T., Meade, D., Kennedy, M., Majer, E., Mlawsky, E., Nakagawa, S., Sophy, M., Pettit, W., Phelps, G., Queen, J., Riahi, A., Robbins, A., Sabin, A., Siler, D., Sonnenthal, E., Stacey, R., Sullivan, P., Robertson-Tait, A., Tang, J., Tiedeman, A., Varun, Villavert, M., Witter, J., 2018, Frontier Observatory for Research in Geothermal Energy: Phase 2B Topical Report, Fallon, NV, SANDIA National Laboratories Report SAND2018-XXXX, 1136 p.

Cockett, R., Kang, S., Heagy, L.J., Pidlisecky, A., and Oldenburg, D.W. "SimPEG, 2015, An open source framework for simulation and gradient based parameter estimation in geophysical applications: Computers & Geosciences, v. 85, p. 142-154.

Jachens, R.C., and Moring, B.C., 1990, Maps of the Thickness of Cenozoic Deposits and the Isostatic Residual Gravity over Basement for Nevada: U.S. Geological Survey Open-File Report 90-404, 15 p.

Kucks, R.P., Hill, P.L., and Ponce, D.A., 2006, Nevada magnetic and gravity maps and data—A website for the distribution of data: U.S. Geological Survey Data Series 234. [http://pubs.usgs.gov/ds/2006/234].

Morrison, R.B., 1964, Lake Lahontan: Geology of Southern Carson Desert, Nevada. Geological Survey Professional Paper 401, U.S. Geological Survey, 165 pages.

Siler, D.L., Hinz, N.H., Faulds, J.E., Ayling, B., Blake, K., Tiedeman, A., Sabin, A., Blankenship, D., Kennedy, M., Rhodes, G., Sophy, M.J., Glen, J.M.G., Phelps, G.A., Fortuna, M., Queen, J., Witter, J.B., 2018, The Geologic and Structural Framework of the Fallon FORGE site. Proceedings of the 43rd Workshop on Geothermal Reservoir Engineering, Stanford University, Stanford, California, February 12-14, 7 pages.

Talwani, M., Worzel, J.L., and Landisman, M.G., 1959, Rapid gravity computations for two-dimensional bodies with application to the Mendocino submarine fracture zone [Pacific Ocean]: Journal of Geophysical Research, v. 64, no. 1, p. 49-59.

U.S. Geological Survey, 1972, Aeromagnetic map of parts of the Lovelock, Reno, and Millett 1 degree by two degrees quadrangles, Nevada: U.S. Geological Survey Open-File Report 72-386.

Witter J.B., Siler D.L., Faulds J.E., Hinz N.H., 2016, 3D Geophysical inversion modelling of gravity data to test the 3D geologic model of the Bradys geothermal area, Nevada, USA: Geothermal Energy, v. 4, no. 14, DOI 10.1186/s40517-016-0056-6.